Using the Ornstein-Uhlenbeck Process for Random Exploration

Johannes Nauta, Yara Khaluf and Pieter Simoens

Department of Information Technology, Ghent University, Ghent, Belgium

Keywords: Brownian Motion, Exploration, Ornstein-Uhlenbeck Process.

Abstract: In model-based Reinforcement Learning, an agent aims to learn a transition model between attainable states. Since the agent initially has zero knowledge of the transition model, it needs to resort to random exploration in order to learn the model. In this work, we demonstrate how the Ornstein-Uhlenbeck process can be used as a sampling scheme to generate exploratory Brownian motion in the absence of a transition model. Whereas current approaches rely on knowledge of the transition model to generate the steps of Brownian motion, the Ornstein-Uhlenbeck process does not. Additionally, the Ornstein-Uhlenbeck process naturally includes a drift term originating from a potential function. We show that this potential can be controlled by the agent itself, and allows executing non-equilibrium behavior such as ballistic motion or local trapping.

1 INTRODUCTION

In autonomous and complex systems, exploration is a necessary component for learning how to act within an unknown environment (Wilson et al., 1996). A widely used approach wherein an agent aims to maximize a cumulative task specific reward is Reinforcement Learning (RL). Specifically, model-based RL includes an alternative (or additional) goal where the reward is not only task specific but tied to learning the transition model between attainable states. Once the model is learnt, the agent can exploit this knowledge to plan the most rewarding actions given a task, making model-based learning approaches display generalization capabilities. Since the agent has no prior knowledge of the environment, it needs to resort to exploration to search and learn within the environment before any exploitation can occur.

Essentially, efficient exploration is a search for novelty, in which the agent should be steered towards previously unvisited states. Model-based learning benefits from efficient exploration because to generate a global transition model all states within the state space first have to be visited. In model-based RL, the novelty increases in sparsity as the agent visits more of the state space. This essentially converts exploration to a problem of sparse target search. Extensive search for sparse targets via random walks is a widely studied subject in the field of ecology (Viswanathan et al., 1999; Bartumeus et al., 2005; Ferreira et al., 2012). However, these approaches execute random walks based on knowing the transition model. Since the transition model is absent in novel environments, these approaches are insufficient for use as an exploration strategy. We therefore aim to use an efficient exploration strategy that visits many different attainable states using random walks that do not require a transition model.

As a first step, we wish to generate Brownian motion through action sampling. Arguably, while Brownian motion as a search strategy is often outperformed by other types of random walks, it is efficient in case of revisitable targets (James et al., 2010) or in the presence of a bias (Palyulin et al., 2014). Hence, we consider action-driven Brownian motion as a stepping stone for further enhancing exploration in the absence of a transition model. Random walks resulting from action sampling have been described in (Lillicrap et al., 2015), where similar to our work the random walk is considered an exploration policy. However, their framework is not suitable for model-learning as well as analytical expressions for the agents' movement are missing.

For a model-learning RL agent, executing Brownian motion is non-trivial, because traditionally the motion is achieved by sampling displacements from a desired distribution. For example, in two dimensions an angle and step-length are sampled and the agent moves accordingly. However, when the transition model is unknown, the agent is unable to determine the action that would result in this target displacement, rendering such sampling procedures obsolete. We therefore introduce an action-sampling framework based on the Ornstein-Uhlenbeck (OU)

59

process (Uhlenbeck and Ornstein, 1930). The OU process allows an agent to realize Brownian motion by sampling actions and without access to a transition model. After convergence, the OU process evolves the agents' velocity according to a Langevin equation with normally distributed random forces. The fact that the agent's velocity follows a Gaussian distribution, gives rise to the Brownian motion.

Additionally, the OU process naturally encompasses a drift term. This drift term can be formulated such that it originates from self-induced potentials by the agent. This allows the agent to change to non-equilibrium motion, which holds promise for replicating other types of random walks. Changing the motion is a necessity for efficiency, since optimal search often interchanges local Brownian motion with long-range displacements (Bartumeus et al., 2005; Ferreira et al., 2012). Such *active Brownian motion* has been studied in biology and physics (Romanczuk et al., 2012), where active Brownian motion results in out-of-equilibrium motion through self-propellation (Volpe et al., 2014; Basu et al., 2018).

The paper is organized as follows. We first characterize random walks and discuss several metrics in Section 2. Then, the OU process is described and analytical expressions for the metrics are obtained in Section 3. We additionally introduce the internal drive and generalize to higher dimensions. The sampling procedure and numerical details are listed in Section 4. Both analytical and empirical results acquired through simulation are shown in Section 5. The paper is concluded with a discussion in Section 6.

2 RANDOM WALKS FOR EXPLORATION

Let us consider an agent as a particle within a Euclidean space. Whereas the ultimate goal of the agent is to learn a transition model that predicts the next state given an action, this paper focuses on the framework that generates random walks for exploration. These need to satisfy a number of requirements. First, the framework needs to be able to handle continuous state and action spaces, since physical control tasks are often continuous in both states and actions. Second, in absence of a transition model, the framework needs to be based on sampling actions. Third, the framework needs to incorporate an intrinsic drive that influences the motion of the agent. The OU process incorporates all three requirements and is therefore an excellent choice for use as an exploration strategy.

2.1 Metrics

Random walks are often characterized by several metrics, mainly the distribution of step-lengths as well as the mean squared displacement. The step-length distribution essentially determines the type of random walk. Brownian motion is recovered when the step-lengths are distributed according to a zero-mean Gaussian. The mean squared displacement $\langle R^2(t) \rangle$ of the agent is an indication of the size of the explored regions of the state space. In one dimension, the mean squared displacement is given by

$$\langle R^2(t) \rangle_{v_0} = \langle (x(t) - x_0)^2 \rangle_{v_0}, \tag{1}$$

where v_0 the velocity and x_0 the position at $t = 0$. The operator $\langle . \rangle_{v_0}$ denotes the ensemble average, which is computed by averaging over many non-interacting agents that all start with the same initial velocity v_0.

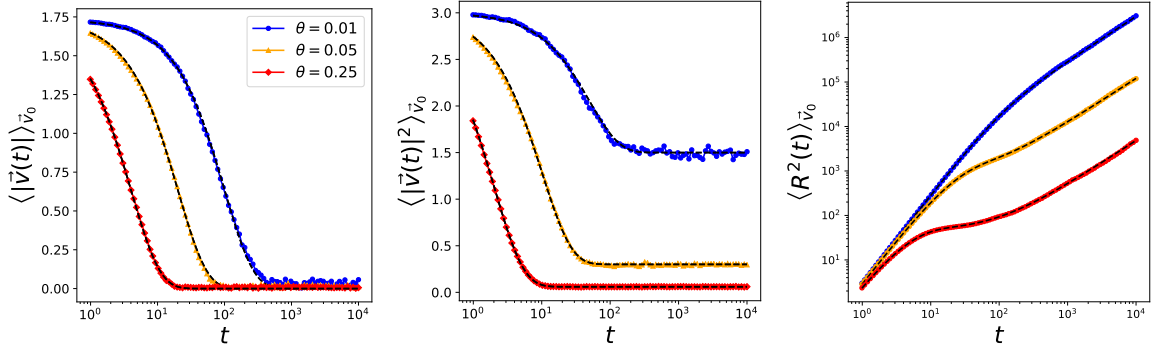## 2.2 Coverage of the State Space

The time evolution of the mean squared displacement is an indication of the efficiency of the coverage of the random walk. It corresponds to different types of diffusion, characterized by a power-law exponent γ, where

$$\langle R^2(t) \rangle_{v_0} \propto t^\gamma, \quad \gamma > 0 \tag{2}$$

Normal diffusion has linear scaling of the mean squared displacement with time, corresponding to $\gamma = 1$. If $\gamma < 1$, the agent undergoes *subdiffusion* and for $\gamma > 1$ *superdiffusion* arises. Since the mean squared displacement is an indication of the explored area of the environment, higher values of γ are generally preferred when the goal is to increase this coverage. However, one should be careful when making conclusions of the random walk based solely on the time evolution of the mean squared displacement. For example, ballistic (straight line) motion is easily regained by simply evolving the agent according to $x = vt$, with a constant velocity v. In this case, it is simple to see that $\gamma = 2$. However, intuitively, ballistic motion does not lead to a homogeneous coverage of the explored environment and thus γ can give a wrong indication of the movement of the agent and should be interpreted with care.

3 THE ORNSTEIN-UHLENBECK PROCESS

In this section, we introduce the reader to the OU process that forms the foundation of the sampling

(a) Ensemble mean of velocity   (b) Ensemble mean of squared velocity   (c) Mean squared displacement

Figure 1: Ensemble averages of the first (a) and second (b) moments of the velocity for the three-dimensional OU process with uncorrelated Brownian noise, for different values of θ. Mean square displacements of the same processes are shown in (c). Note the convergence to $\gamma \approx 1$ when t increases. In this case, $\vec{\mu} = (0,0,0)^T$, $\vec{v}_0 = (1,1,1)^T$, $\vec{x}_0 = (0,0,0)^T$. Black dotted lines indicate the analytical result.

scheme that is presented in Section 4. The OU process is a well-known diffusion process described by a Langevin equation (Uhlenbeck and Ornstein, 1930). In one dimension, the position of the agent starting at x_0 is given by

$$x(t) = x_0 + \int_0^t v(s)\,ds \qquad (3)$$

The velocity is derived from Newton's law and has the following form

$$m\frac{dv(t)}{dt} = -m\theta v(t) + F_U(x) + B(t), \qquad (4)$$

where θ denotes a friction coefficient, $F_U(x)$ the external force and $B(t)$ the stochastic force acting on the agent with mass m. The ensemble average of the velocity is given by

$$\langle v(t)\rangle_{v_0} = v_0 e^{-\theta t} + \mu\left(1 - e^{-\theta t}\right), \quad \mu = \frac{F_U(x)}{m\theta} \quad (5)$$

which converges to the drift μ in the time limit $t \to \infty$. The second moment is given by

$$\langle v^2(t)\rangle_{v_0} = \left[v_0 e^{-\theta t} + \mu\left(1 - e^{-\theta t}\right)\right]^2 + \frac{g}{2\theta m^2}\left(1 - e^{-2\theta t}\right), \qquad (6)$$

where g is the correlation strength of the stochastic forces, indicating a time-range over which the stochastic forces are correlated. In the large-time limit, the second moment equals $\mu^2 + g/2\theta m^2$, given that $F_U(x) = F_U$ a constant. In contrast with the first moment, this includes a dependency on the friction coefficient θ in the large-time limit, generating an offset due to friction.

Next we wish to determine the mean squared displacement of the ensemble in the presence of a constant external force

$$\langle R^2(t)\rangle_{v_0} = \left[\frac{v_0 - \mu}{\theta}\left(1 - e^{-\theta t}\right) + \mu t\right]^2 + \frac{g}{m^2\theta^2}\left[t + \frac{1}{2\theta}\left(4e^{-\theta t} - e^{-2\theta t} - 3\right)\right], \qquad (7)$$

which in the large-time limit equals

$$\lim_{t\to\infty}\langle R^2(t)\rangle_{v_0} = \left(\frac{v_0 - \mu}{\theta} + \mu t\right)^2 + \frac{g}{m^2\theta^2}\left(t - \frac{3}{2\theta}\right) \qquad (8)$$

When the drift equals 0 we obtain the famous result of Einstein, namely that the mean squared displacement scales linearly with time, i.e. $\langle R^2(t)\rangle_{v_0} \propto t$ (Einstein, 1905). When the drift is non-zero, we obtain $\langle R^2(t)\rangle_{v_0} \propto t^2$. Furthermore, $v(t)$ is normally distributed when $t \to \infty$, with mean μ and variance $\langle v^2(t)\rangle_{v_0} - \langle v(t)\rangle_{v_0}^2$. As a result, displacements of the position $x(t)$ are normally distributed, effectively replicating Brownian motion when $\mu = 0$.

3.1 Origin of Internal Drift

In physics, the drift μ is typically regarded as an extrinsic effect, uncontrollable by the agent. However, it is important to note that the sampling of the forces (and thus the velocities) is performed by the agent itself. Thus, applying an external drift to a passive agent is the same as applying an *internal drift* to an active agent. As motivated in the introduction, this internal drift can act similar to a curiosity signal (Hafez et al., 2017), where the agent can undergo a drastic transition or stay close to its current location depending on its intentions.
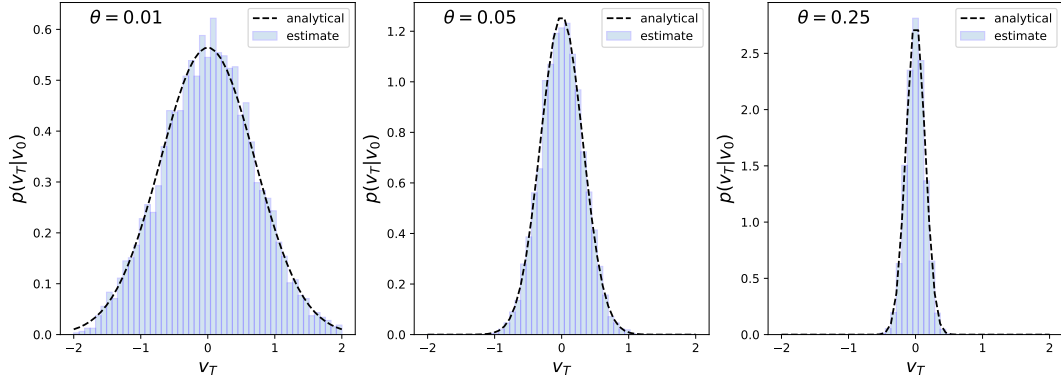
Figure 2: Velocity distributions for the one-dimensional OU process at $T = n\Delta t$, for different values of θ, $\mu = 0$, $v_0 = 1$, $m = 1$. Note that the distribution is Gaussian with mean $\langle v(T) \rangle_{v_0} = \mu$ and variance $\langle v^2(T) \rangle_{v_0} - \langle v(T) \rangle_{v_0}^2 = \frac{g}{2\theta m^2}$.

Analytically, F_U can be written as the derivative of a potential $U(x,t)$, giving us the Langevin equation for the velocity as

$$m\frac{dv(t)}{dt} = -m\theta v(t) - \frac{d}{dx}U(x,t) + B(t), \quad (9)$$

where the minus sign appears through the resulting intrinsic force $F_U = -dU/dx$. This equation indicates that the drift can be both position-dependent and time-dependent. Note that the performed analysis to compute the ensemble averages does only holds when the potential is position-dependent, not time-dependent. Since the velocity converges to $\mu = F_U/m\theta$ in the large-time limit (see Eq. (5)), an agent can thus actively induce non-equilibrium behavior by manipulating the self-induced potential. For instance, an appropriate choice of potential will allow the agent to "trap" itself in a region or conversely to realize ballistic (straight line) motion. In the remainder of this paper, we shall only consider position dependent potentials.

3.2 Generalization to Multiple Dimensions

In RL, action spaces are often high-dimensional. For example, a robotic arm can have multiple joints on which forces can be exerted. Therefore, if we wish to enable model-based learning for agents with many degrees of freedom, we need to extend the OU process to higher dimensions. This generalization is straightforward by considering the n-dimensional Langevin equation

$$\vec{x}(t) = \vec{x}_0 + \int_0^t \vec{v}_s\, ds, \quad (10)$$

$$m\frac{d\vec{v}(t)}{dt} = -m\theta\vec{v}(t) + \vec{F}_U + \vec{B}(t), \quad (11)$$

Solving the Langevin equation and computing the ensemble average again gives

$$\langle \vec{v}(t) \rangle = \vec{v}_0 e^{-\theta t} + \vec{\mu}(1 - e^{-\theta t}), \qquad \vec{\mu} = \frac{\vec{F}_U}{m\theta} \quad (12)$$

When $t \to \infty$, the ensemble average of the velocity again converges to the external drift $\vec{\mu}$ since for each dimension holds $\lim_{t \to \infty} \langle v_i(t) \rangle_{\vec{v}_0} = \mu_i$. The mean squared displacement depends on the correlation matrix $\Sigma^{v(t)}$. The random forces are considered uncorrelated if the noise vector $\vec{B}(t) = (B_1(t), B_2(t), \ldots B_n(t))$ is an n-dimensional vector consisting of independent Wiener processes (Ibe, 2013), i.e.

$$\langle B_i(t)B_j(t') \rangle = g\delta_{ij}\delta(t - t'), \quad (13)$$

where δ_{ij} is the Kronecker delta and $\delta(t - t')$ the Dirac delta function. The covariance matrix of the velocity is given by

$$\Sigma_{ij}^{v(t)} = \frac{g\delta_{ij}}{2\theta m^2}\left(1 - e^{-2\theta t}\right), \quad (14)$$

which is a diagonal matrix. Thus our n-dimensional velocity is distributed according to a multivariate Gaussian distribution with mean $\vec{\mu}$ and diagonal covariance matrix $\Sigma^{v(t)}$. For computing the mean squared displacement we define $\vec{r}(t) = \vec{x}(t) - \vec{x}_0$, which gives

$$R^2(t) = |\vec{r}(t)|^2 = \sum_{i=1}^n r_i^2(t), \quad (15)$$

which is simply the sum of the squared displacements in each dimension (i.e. the square of the Euclidean distance between $\vec{x}(t)$ and $\vec{x}_0$). Substituting the velocity of Eq. (11) and squaring we have

$$\langle R^2(t) \rangle_{\vec{v}_0} = \sum_{i=1}^n \left\{ \left[\frac{v_i^0 - \mu_i}{\theta}\left(1 - e^{-\theta t}\right) + \mu_i t\right]^2 + \frac{gt}{m^2\theta^2}\left(t + \frac{1}{2\theta}\left[4e^{-\theta t} - e^{-2\theta t} - 3\right]\right) \right\}, \quad (16)$$

which is the sum of the mean squared displacement in all dimensions, where each dimension has the same expression as Eq. (7). This result is expected, since we defined the *n*-dimensional noise vector having independent components. Therefore, each dimension is undergoing Brownian motion, with the mean squared displacement being the sum of displacements in each dimension. Brownian motion is often modelled using correlated noise (i.e. non-diagonal elements of the covariance matrix are non-zero), however careful analysis of such systems are considered future work.

4 SAMPLING PROCEDURE

To realize Brownian motion in the state space $\mathcal{S}$ at discretized points in time with time-steps Δt, an agent with mass $m = 1$ will sample forces ξ from a normal distribution ξ with mean 0 and standard deviation Δt, $\mathcal{N}(0, \Delta t)$. This results in a time-discretization of Eq. (10) and Eq. (11) of the velocity and position in each dimension i:

$$v_{t+\Delta t, i} = v_{t,i}(1 - \theta \Delta t) + \mu_i + \xi_{t,i}, \qquad (17)$$

$$x_{t+\Delta t, i} = x_{t,i} + v_{t+\Delta t, i}\Delta t \qquad (18)$$

Setting the standard deviation of $\xi_{t,i}$ to Δt also defines the correlation strength of stochastic driving force, namely $\langle B^2(t) \rangle = g = \Delta t$. This means that the stochastic forces are only correlated within a time range Δt, defining a Wiener process. Ensemble averages of the (squared) velocity and the mean squared displacement are computed over an ensemble of $N = 1000$ non-interacting agents, unless stated otherwise. Since our interest lies mostly in the large-time limit, we evolve Eq. (17) and Eq. (18) for $n = 10^6$ steps, where $\Delta t = 0.01$. In multiple dimensions, we compute the ensemble average of the absolute value of the velocity, i.e. the length of the velocity vector,

$$|\vec{v}(t)| = \sqrt{\sum_{i=1}^{D} v_i^2(t)}, \quad |\vec{v}^2(t)| = \sum_{i=1}^{D} v_i^2(t), \qquad (19)$$

where D is the number of dimensions. The power-law exponent of the mean squared displacement can be numerically approximated by discretizing time with increments s:

$$\gamma(t) \approx \frac{\log\left(\langle R^2(t+s)\rangle_{v_0}\right) - \log\left(\langle R^2(t)\rangle_{v_0}\right)}{\log(t+s) - \log(t)}, \qquad (20)$$
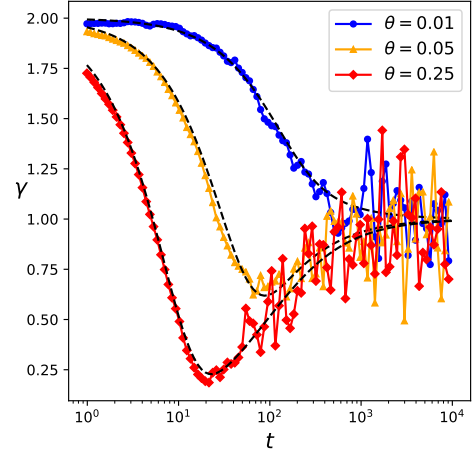
where $\log(\cdot)$ the natural logarithm.

Figure 3: Power-law exponent γ of the three-dimensional OU process with uncorrelated Brownian noise for $\mu = 0$, $v_0 = 1$, $x_0 = 0$. For large t, $\gamma \approx 1$, indicating standard diffusion, i.e. Brownian motion. Black dotted lines indicate the analytical result. Note that at $t \to \infty$, $\gamma \to 1$ regardless of θ. Large deviations are due to numerical computation of the derivative.

5 RESULTS

We verify the analytical results and build upon the results to display active particle steering is able to effectively guide the agent to undergo non-equilibrium behavior. In Section 5.1, we first validate whether we are indeed able to realize Brownian motion through action sampling. In Section 5.2, we show an agent can change the distribution of the state space exploration trajectory by applying different potentials.

5.1 Brownian Motion

We investigate the numerical simulations of the three-dimensional OU process in the absence of a drift term ($\mu = 0$), described through Eqs. (17) and (18). We aim to verify that each agent is indeed undergoing Brownian motion through measuring the metrics mentioned in Section 2.

5.1.1 Velocity Distribution

The velocity distribution is defined through the first and second moment. The results for both moments are displayed in Figs. 1a, 1b. Excellent agreement between the analytical and numerical solutions is observed. For large t, the first moment of the velocity tends towards the extrinsic drift $\mu = 0$, whereas the second moment converges to a value that depends on θ. For both moments, the strength θ determines
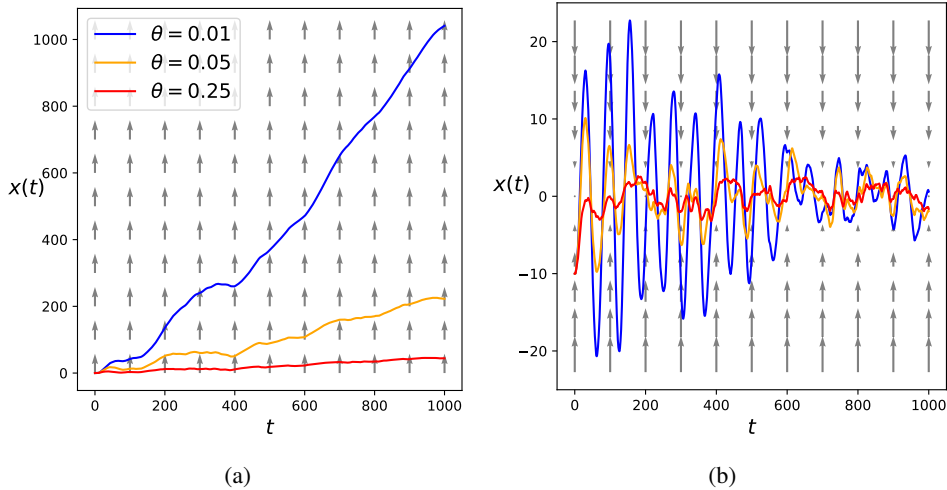
Figure 4: Sample trajectories of the one-dimensional Brownian particle in different potentials for different strengths of the OU process, for $n = 10^5$ steps, $\Delta t = 0.01$. The arrows indicate the potential $U(x)$. (a) $U(x) = -ax$, for $x_0 = 0$, $a = 0.01$, (b) $U(x) = ax^2$, for $x_0 = -10$, $a = 0.01$.

the convergence time of the process through a typical time $\tau = \theta^{-1}$. In the large time limit, the velocity is Gaussian (Uhlenbeck and Ornstein, 1930) around $\mu = 0$. This is indicated in Fig. 2, where the empirical velocity at $T = n\Delta t$ is indeed Gaussian. This means that, for large t, the agent is sampling from a (multivariate) Gaussian.

5.1.2 Mean Squared Displacement

The mean squared displacement is plotted in Fig. 1c. The analytical and numerical results are again in excellent agreement. The power-law coefficient of the mean squared displacement, calculated by means of Eq. (20), is plotted in Fig. 3. Note the transition between super-linear scaling ($\gamma > 1$) and linear scaling ($\gamma = 1$) around the typical time $\tau = \theta^{-1}$. Furthermore, for large θ, there exists a time window of subdiffusion ($\gamma < 1$) arising from the slowing down of the agents due to a large friction coefficient θ.

5.2 Active Motion

Next we shall consider two elementary potential functions $U(x)$ to demonstrate how an agent can induce other types of (non-equilibrium) motion. Ballistic motion is able to induce large displacements, desired if the agent wishes to visit far away regions of the state space. In contrast, trapping the agent around a certain state enables local exploration where movement is bound to a small area. Combining large displacements and local trapping can give rise to continuous time random walks (Volpe and Volpe, 2017). Additionally, the combination of these two potentials may enable replication of many different continuous time

random walks, as these are often a combination of local Brownian motion and long, correlated movement (Zaburdaev et al., 2015). For visual purposes, we have chosen to illustrate all results in one dimension, however generalization to multiple dimensions is trivial (see Section 4).

5.2.1 Linear Potential

Let us consider a linear potential $U = -ax$ such that

$$\frac{dv(t)}{dt} = -\theta v(t) + a + B(t) \qquad (21)$$

A sample trajectory is shown in Fig. 4a. For lower values of θ, the agent experiences less friction and thus larger deviations are observed. This indicates the trivial result that a frictionless particle exhibits higher displacements within the same time. In the large-time limit, we know that the ensemble mean of the velocity converges to the drift $\mu = a$. The result is that the Brownian particle will move with a close to constant velocity when time increases (see Figs. 6a, 6b), resulting in the visible straight line displacement with respect to time as seen in Fig. 4. Thus, by using a linear potential, we are able to actively steer the agent to undergo ballistic motion corresponding to $x = vt$ with a constant velocity $\mu = a/\theta$ in the large time limit. As shown in Fig. 5a, the mean squared displacement indeed evolves according to $\gamma \approx 2$ for all θ when t is large.

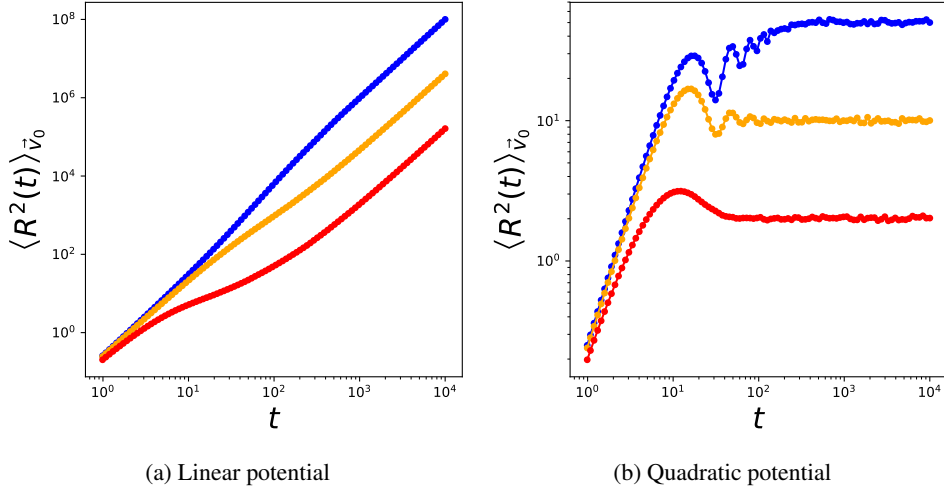(a) Linear potential   (b) Quadratic potential

Figure 5: Mean squared displacement of the OU process in different potentials, for different values of θ. Here, $v_0 = \frac{1}{2}$, $x_0 = 0$, $a = 0.01$. (a) Given a linear potential $U = -ax$, we note that the mean squared displacement scales according to $\gamma \approx 2$. (b) Indicates trapping of the particle for $U = ax^2$ ($\gamma = 0$) where θ influences the average displacement at which the particle becomes trapped.

5.2.2 Quadratic Potential

Let us consider a quadratic potential $U = ax^2$ such that

$$\frac{dv(t)}{dt} = -\theta v(t) - ax + B(t) \qquad (22)$$

By applying this potential, we expect that the agent can trap itself close to the minimum of this potential at $x = 0$, with θ again describing the influence of friction. High friction results in fast trapping of the agent, whereas low friction indeed displays fluctuations around the minimum of the potential with significantly larger times necessary before effective trapping occurs (see Fig. 4). For small θ, the agent is able to drift further away from the minimum of the potential due to overshooting the minimum. The mean squared displacement is plotted in Fig. 5 for different values of θ. After some time, the agent indeed becomes trapped, indicated by a stagnation of the mean squared displacement and the mean velocity (see Figs. 5b, 6c). The friction coefficient of the OU process encodes deviations from the mean, meaning that small values of θ indicate a higher variance for the velocity distribution, as indicated in Fig. 6d. This induces, on average, further displacements from the minimum of the potential at $x = 0$. The first and second moments of the velocity converge to different values for different θ.

(a)   (b)

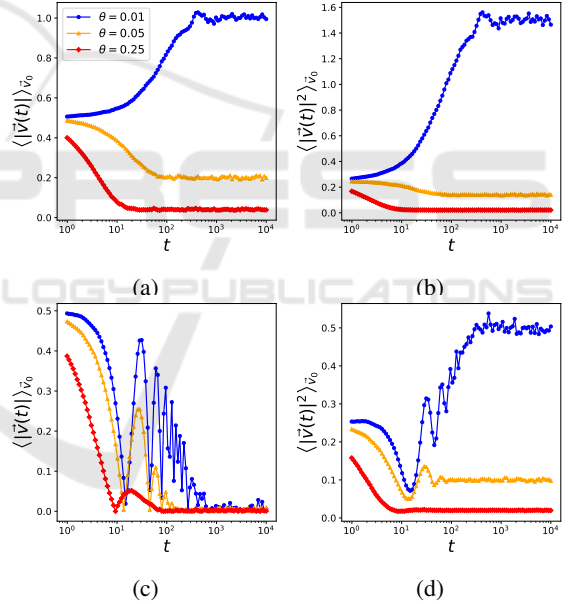(c)   (d)

Figure 6: Ensemble average of first and second moments of the velocity for the one-dimensional OU process in different potentials, for different values of θ. Colours corresponding to different θ are shown in the legend in (a). In all cases, $v_0 = \frac{1}{2}$, $x_0 = 0$, $a = 0.01$. a) + (b): Linear potential $U = -ax$. (c) + (d): Quadratic potential, $U = ax^2$.

6 CONCLUSION

Learning a state transition model is a prerequisite of any model-based RL control paradigm. To learn such a model efficiently, an agent must efficiently explore the state space. In this paper, we presented an ap-

proach that is based on the OU process to realize active guidance of an agent through state space by sampling velocities instead of displacements. We have assumed zero knowledge of the transition model, since this is generally the case in most model-based RL settings. The OU process evolves the agents' velocity according to a Langevin equation, where in the large-time limit the sampled velocities follow a Gaussian distribution. Additionally, the model allows the agent to influence the action sampling scheme (and thus its motion pattern) by means of a self-induced potential function. One key advantage of our approach is that we can derive closed-form analytical expressions.

In this paper, we have assumed that the transition model remains unknown, even after the agent has explored the environment for some time. However, when model-based learning is considered, the agent often builds its knowledge in a incremental, iterative fashion. In order to account for this, in future work we will study the effects of making the strength θ time-dependent as well as changing the intrinsic drift term μ in reaction to encountered novelty. This generates a framework wherein the intrinsic drive originates from extrinsic sources or observations, resembling an intuitive implementation of a curious agent.

Furthermore, acquiring similar analytical expressions for different types of random walks is highly desirable. In particular, we wish to focus on a Lévy walk (Zaburdaev et al., 2015). In a Lévy walk, the displacements are sampled from a power law, interchanging local displacements with long time-correlated displacements within the environment. Using different potentials, one can most likely replicate Lévy-like behavior through the process described in this work. One could alternatively use a different formulation of the underlying noise scheme, i.e. sample directly from the desired distribution. This possibly give rise to Lévy walks and might further enhance exploration of an environment (Bartumeus et al., 2005; Ferreira et al., 2012).

This work indicates a stepping stone in simulating random walks for exploration. Enabling random walks in the absence of a transition model might prove beneficial for model-based RL, even opening the doors to more efficient sampling schemes that improve learning in continuous state spaces.

REFERENCES

Bartumeus, F., da Luz, M. G. E., Viswanathan, G. M., and Catalan, J. (2005). Animal search strategies: a quantitative random-walk analysis. Ecology, 86(11):3078–3087.

Basu, U., Majumdar, S. N., Rosso, A., and Schehr, G.

(2018). Active brownian motion in two dimensions. arXiv preprint arXiv:1804.09027.

Einstein, A. (1905). Investigations on the theory of the brownian movement. Ann. der Physik.

Ferreira, A., Raposo, E., Viswanathan, G., and da Luz, M. (2012). The influence of the environment on lévy random search efficiency: Fractality and memory effects. Physica A: Statistical Mechanics and its Applications, 391(11):3234 – 3246.

Hafez, M. B., Weber, C., and Wermter, S. (2017). Curiosity-driven exploration enhances motor skills of continuous actor-critic learner. In 2017 Joint IEEE International Conference on Development and Learning and Epigenetic Robotics (ICDL-EpiRob), pages 39–46.

Ibe, O. C. (2013). Elements of Random Walk and Diffusion Processes. Wiley Publishing, 1st edition.

James, A., Pitchford, J. W., and Plank, M. (2010). Efficient or inaccurate? analytical and numerical modelling of random search strategies. Bulletin of Mathematical Biology, 72(4):896–913.

Lillicrap, T. P., Hunt, J. J., Pritzel, A., Heess, N., Erez, T., Tassa, Y., Silver, D., and Wierstra, D. (2015). Continuous control with deep reinforcement learning. CoRR, abs/1509.02971.

Palyulin, V. V., Chechkin, A. V., and Metzler, R. (2014). Lévy flights do not always optimize random blind search for sparse targets. Proceedings of the National Academy of Sciences, 111(8):2931–2936.

Romanczuk, P., Bär, M., Ebeling, W., Lindner, B., and Schimansky-Geier, L. (2012). Active brownian particles. The European Physical Journal Special Topics, 202(1):1–162.

Uhlenbeck, G. E. and Ornstein, L. S. (1930). On the theory of the brownian motion. Phys. Rev., 36:823–841.

Viswanathan, G. M., Buldyrev, S. V., Havlin, S., Da Luz, M., Raposo, E., and Stanley, H. E. (1999). Optimizing the success of random searches. Nature, 401(6756):911.

Volpe, G., Gigan, S., and Volpe, G. (2014). Simulation of the active brownian motion of a microswimmer. American Journal of Physics, 82(7):659–664.

Volpe, G. and Volpe, G. (2017). The topography of the environment alters the optimal search strategy for active particles. Proceedings of the National Academy of Sciences, 114(43):11350–11355.

Wilson, S. W. et al. (1996). Explore/exploit strategies in autonomy. In Proc. of the Fourth International Conference on Simulation of Adaptive Behavior: From Animals to Animats, volume 4, pages 325–332.

Zaburdaev, V., Denisov, S., and Klafter, J. (2015). Lévy walks. Reviews of Modern Physics, 87(2):483.